

Probing the nuclear density with hadrons: Feasibility and limitations

H. O. Meyer

Institut für Physik, University of Basel, CH-4056 Basel, Switzerland

(Received 21 November 1977)

The derivation of nuclear neutron distributions from hadron-nucleus scattering data is critically examined. Using the Glauber model, we investigate how the total and differential cross sections depend on specific properties of the radial nucleon densities $\rho_N(r)$ of the target nucleus. Emphasis is placed on the interpretation of hadron-nucleus total cross sections. As to the deduction of r.m.s radii from total cross-section measurements only, we find that a large systematic error arises from the *a priori* unknown shape of $\rho_N(r)$. This error can be reduced if physically justified constraints are imposed on $\rho_N(r)$. In many published analyses, however, the constraint on $\rho_N(r)$ has been of mathematical origin since only density distributions of a certain shape (e.g., Fermi distributions) have been used. As an example, our findings are applied to two recent pion-nucleus total cross section experiments. It is also shown that earlier attempts to avoid a mathematical constraint on $\rho_N(r)$ must be viewed with reservations.

[NUCLEAR STRUCTURE Hadron-nucleus scattering, deduction of matter
radius, model dependence.]

I. INTRODUCTION

Radial distributions of protons in nuclei are known much more precisely than those of neutrons; the former can be investigated via the electromagnetic interaction, while for the latter we depend on processes involving the strong interaction (with the exception of one special case¹). Methods to study nuclear neutron distributions are listed, e.g., in Table I of Ref. 2. Among these methods is the scattering of hadrons from nuclei: Experiments with various probes at many bombarding energies and for different nuclei have been analyzed³⁻¹³ in terms of the (unknown) neutron density distribution $\rho_n(r)$. Obviously, such a procedure is somewhat uncertain at present because it depends on a reliable model for the projectile-nucleus interaction, such that $\rho_n(r)$ can be considered the only unknown quantity. However, for medium- and high-energy hadron scattering this difficulty is not very serious where the data are well explained by theories which start from the density distributions $\rho_n(r)$ and $\rho_p(r)$ and the interaction of the projectile with individual free nucleons (e.g., Glauber model, Kisslinger optical model).

If one postulates the validity of such a model and assumes $\rho_p(r)$ to be known (from elastic electron scattering), one can search for a $\rho_n(r)$ which leads to agreement between the calculated observables and the experimental quantities. In such an analysis, $\rho_n(r)$ is commonly described by a function of r with as few parameters as needed to fit the data. Often a Fermi distribution¹⁴ is chosen^{8-13,15} for $\rho_n(r)$ which, beside the (fixed) normalization, depends on two parameters, e.g., the skin thickness

z and the half-density radius c (or the rms radius $\langle r^2 \rangle^{1/2}$). Sometimes a third parameter w is introduced.¹⁴

Using Fermi distributions it has long been realized⁷⁻⁹ that the scattering observables calculated within various interaction models depend strongly on $\langle r^2 \rangle^{1/2}$ but only weakly on z . It is common practice to jump from this fact to the conclusion that the method just described is equivalent to a determination of the rms radius of the true neutron distribution. It is not clear, however, if the true neutron density actually is close enough to a Fermi distribution. The selective sensitivity of the data to the rms radius could well be simulated by the choice of a particular mathematical form for $\rho_n(r)$ with only a few arbitrary degrees of freedom.

This difficulty has first been recognized in electron scattering for which various so-called model-independent densities (e.g., Ref. 16) have been proposed. For a few cases of hadron scattering, investigations along similar lines have been reported recently¹⁷⁻¹⁹ (for details see Sec. IV).

The purpose of the present paper is to demonstrate which particular properties of $\rho_n(r)$ are determined by hadron-nucleus scattering experiments, and to explore the impact of a model for $\rho_n(r)$ (e.g., Fermi distribution) on conclusions about $\rho_n(r)$ deduced from such data. To keep the necessary formalism to a minimum we make use of the Glauber model in a simple approximation from which in Sec. II we derive the dependence of scattering observables on the nuclear densities.

In Sec. III this formalism is applied to the case of total cross sections. This is exemplified by a

reevaluation of some findings of recent experiments. Simple consequences of our results regarding angular distributions of the differential elastic cross section are given in Sec. IV, followed by a discussion of model-independent analyses available at present.

II. DEPENDENCE OF SCATTERING OBSERVABLES ON NUCLEAR DENSITIES, INTERACTION MODEL

In the following, the *sensitivity* of an interaction model on details of the input density distributions is investigated. For this purpose it is sufficient to use a simple (transparent) formalism. The amplitude for the scattering of a projectile x from a nucleus in the framework of the Glauber multiple scattering theory^{20,21} (optical limit) can be written as

$$F_x(q) = ik \int_0^\infty J_0(qb) (1 - e^{-G_x(b)}) b db. \quad (1)$$

Here, k is the projectile momentum in the projectile-nucleus c.m. system, b is the impact parameter, and $q = 2k \sin \frac{1}{2} \theta_{c.m.}$ the transferred momentum. We assume the nucleus to be spherically symmetric and neglect the spin of projectile and target. The "elementary" amplitude for the scattering of the projectile x from a free nucleon N (n or p) is given by

$$f_{xN}(q) = \frac{ik}{4\pi} \sigma_{xN} (1 - i\epsilon_{xN}) \exp(-\frac{1}{2} q^2 \beta_{xN}^2) \quad (2)$$

with σ_{xN} the total projectile-nucleon cross section and ϵ_{xN} the ratio of real to imaginary part of the projectile-nucleon forward amplitude $f_{xN}(0)$. For the moment we assume a zero-range interaction, i.e., we use $\beta_{xN}^2 = 0$ for the slope parameter in Eq. (2). One then obtains for the phase function ("eikonal") $G_x(b)$ in Eq. (1):

$$G_x(b) = \sum_{N=n,p} \sigma_{xN} (1 - i\epsilon_{xN}) S_N(b). \quad (3)$$

The thickness of the target nucleus at a given impact parameter is measured by

$$S_N(b) = \int_b^\infty \rho_N(r) (r^2 - b^2)^{-1/2} r dr. \quad (4)$$

The observables we want to discuss are the elastic differential cross section

$$d\sigma_x(q)/d\Omega = |F_x(q)|^2, \quad (5)$$

the total cross section

$$\begin{aligned} \sigma_{\text{tot}}^x &= (4\pi/k) \text{Im} F_x(0) \\ &= 4\pi \int_0^\infty (1 - \text{Re} e^{-G_x(b)}) b db, \end{aligned} \quad (6)$$

and the total reaction cross section (i.e., the total

minus the total elastic cross section)

$$\sigma_{\text{tot},r}^x = 2\pi \int_0^\infty (1 - |e^{-G_x(b)}|^2) b db. \quad (7)$$

Given the elementary amplitudes (σ_{xN} , ϵ_{xN} , $N = n$ or p), the observables can be calculated from the neutron and proton density distributions $\rho_n(r)$ and $\rho_p(r)$.

We assume that the *true* densities $\rho_{n0}(r)$ and $\rho_{p0}(r)$ are known. Any other density different from $\rho_{N0}(r)$ is described by $\Delta\rho_N(r)$ such that

$$\Delta\rho_N(r) = \rho_N(r) - \rho_{N0}(r). \quad (8)$$

We define the generalized moment

$$\langle g(r) \rangle_{\Delta\rho_N} \equiv 4\pi \int_0^\infty r^2 g(r) \Delta\rho_N(r) dr \quad (9)$$

and require the same normalization for $\rho_N(r)$ as for $\rho_{N0}(r)$, i.e.,

$$\langle 1 \rangle_{\Delta\rho_N} = 0. \quad (10)$$

Having set the stage, we turn to the crucial step, calculating the changes $\Delta F_x(q)$, $\Delta\sigma_{\text{tot}}^x$, and $\Delta\sigma_{\text{tot},r}^x$ caused by an increment $\Delta\rho_N(r)$ in one of the nucleon distributions. In this way we investigate how well one can experimentally detect the difference between the true nucleon distribution $\rho_{N0}(r)$ and a $\rho_N(r)$ assumed in the analysis. Expanding the scattering amplitude Eq. (1) in $\Delta S_N(b) = S_N(b) - S_{N0}(b)$ and retaining only terms linear in $\Delta S_N(b)$ [thus in fact limiting $\Delta\rho_N(r)$ to small values] yields

$$\Delta F_x(q) = 4\pi f_{xN}(0) \int_0^\infty r^2 \Delta\rho_N(r) W(r, q) dr \quad (11)$$

with

$$W_x(r, q) = \int_0^r J_0(bq) e^{-G_x(b)} (r^2 - b^2)^{-1/2} \frac{b}{r} db. \quad (12)$$

Expanding the Bessel function in Eq. (12) leads to

$$\Delta F_x(q) = f_{xN}(0) \sum_{j=0}^\infty q^{2j} \frac{(-1)^j}{(2j+1)!} \langle r^{2j} A_j^x(r) \rangle_{\Delta\rho_N}, \quad (13)$$

where

$$A_j^x(r) = \frac{(2j+1)!!}{(2j)!!} \int_0^1 \xi^{2j+1} e^{-G_x(r\xi)} (1 - \xi^2)^{-1/2} d\xi \quad (14)$$

and, according to Eq. (6),

$$\Delta\sigma_{\text{tot}}^x = \sigma_{xN} \text{Re} \langle A_0^x(r) \rangle_{\Delta\rho_N}. \quad (15)$$

For the increment in the total reaction cross section an analogous derivation, starting from Eq. (7), yields

$$\Delta\sigma_{\text{tot},r}^x = \sigma_{xN} \langle B^x(r) \rangle_{\Delta\rho_N} \quad (16)$$

with

$$B^x(r) = \int_0^1 \xi e^{-2 \operatorname{Re} G_x(r\xi)} (1 - \xi^2)^{-1/2} d\xi. \quad (17)$$

As an example, consider the limiting case of a "transparent" nucleus ($\sigma_{xN} \rightarrow 0$, $\epsilon_{xN} \rightarrow 0$). It follows that $A_j^x(r) \rightarrow 1$ and $B^x(r) \rightarrow 1$ for all j and r , and $\Delta F_x(q)$ takes the form

$$\Delta F_x(q) = f_{xN}(0) \left\{ -\frac{q^2}{6} \langle r^2 \rangle_{\Delta \rho_N} + \frac{q^4}{120} \langle r^4 \rangle_{\Delta \rho_N} - + \dots \right\}. \quad (18)$$

Because of the normalization condition [Eq. (10)] there is no q -independent term in the expansion. Therefore, the changes $\Delta F_x(q=0)$, $\Delta \sigma_{\text{tot}}^x$, and $\Delta \sigma_{\text{tot},r}^x$ vanish. This means that the corresponding observables only depend on the normalizations of $\rho_n(r)$ and $\rho_p(r)$. Consequently, only if there are regions in r where the radial weights $A_0^x(r)$ and $B^x(r)$ differ substantially from unity is it possible that σ_{tot}^x or $\sigma_{\text{tot},r}^x$ depend on the nucleon distribution in a nontrivial way. This condition is met for hadron-nucleus scattering as will be seen from a discussion of $A_0^x(r)$ and $B^x(r)$ in Sec. III.

For the sake of simplicity, we have introduced several approximations in the formalism described so far. For a detailed analysis this simple model would have to be corrected for a number of effects.²² However, if we only attempt to discuss the influence of a small change of the nucleon distribution we may neglect these corrections. In addition, the approximations used are not unreasonable. This can be seen, e.g., from the fact that for the ⁴⁸Ca-⁴⁰Ca differences of π total cross sections in the (3,3) resonance region, the simple model described here yields virtually the same answer as more sophisticated interaction models (see Fig. 2 of Ref. 7). This is not surprising, since it can be seen that those impact parameters which contribute most to the calculated difference in σ_{tot}^x belong to trajectories sampling the low density region of the nucleus, where most of the higher-order effects (e.g., from pair correlations) are small anyhow. This argument still holds for projectiles with spin, since it has been shown that the spin-orbit interaction leads to rather small corrections.²²

Nevertheless, in the following, we inspect some of the approximations made so far, especially since they can affect the first term in the multiple scattering expansion.

One such approximation has been the omission of the slope parameter β of Eq. (2), thus neglecting the finite range of the projectile-nucleon interaction. A second one enters if the nucleon densities of Eq. (4) are to be compared with the prediction

of an independent-particle model. This "c.m. effect" has been discussed²³ for the harmonic oscillator. Both effects mentioned above result in corrections to the nuclear form factor. To a good approximation they can be taken into account simultaneously²⁴ by evaluating Eq. (4) with densities $\rho_N(\vec{r})$ which are the independent-particle model point nucleon densities $\rho_N'(\vec{r} - \vec{r})$ folded with a function

$$\phi(\vec{r}) = \exp\left(-\frac{\vec{r}^2}{2\beta_{xN}^2 - a^2/A}\right), \quad (19)$$

where a denotes the oscillator parameter. These two corrections obviously can be applied by an appropriate modification of the input densities $\rho_N(r)$; thus they tend to be unimportant in cases where differences $\Delta \rho_N(r)$ of nucleon densities are considered.

Since most hadronic scattering data involve charged projectiles it is necessary to include the electromagnetic interaction which has also been neglected so far. Various methods to do this in the framework of the Glauber model have been proposed.^{20,25} For the purpose of this paper, it suffices to mention an approximate method for taking into account the Coulomb interaction in the case of total cross sections. To arrive at the usually quoted experimental σ_{tot}^x , terms containing the pure Coulomb amplitude f_C are subtracted from the directly observable quantities.⁷ However, the resulting σ_{tot}^x still contains electromagnetic effects which can be estimated by considering the distortion of the wave function of the incident charged projectile in the Coulomb field of the nucleus. A semiclassical treatment for pion-nucleus scattering²⁶ leads to

$$\sigma = (1 + \delta)^{-2} \sigma_0, \quad (20)$$

where σ stands for either the total, total elastic, or total reaction cross section and σ_0 for the corresponding quantities in the absence of the Coulomb interaction. The parameter δ is given by Eq. (2) of Ref. 26. This semiclassical Coulomb correction satisfactorily explains, e.g., experimental $\pi^+ - \pi^-$ total cross-section differences in the (3,3) resonance region.^{27,28}

III. TOTAL CROSS SECTION

Measured hadron-nucleus total cross sections σ_{tot}^x or $\sigma_{\text{tot},r}^x$ have been used to extract information on the matter distribution, or—with $\rho_p(r)$ known—the neutron distribution $\rho_n(r)$. The list of experiments which have been exploited in this way includes $\sigma_{\text{tot}}^{\pi^+}$ (isotopic differences) at 0.1–0.25 GeV on ^{48,44,40}Ca⁷; $\sigma_{\text{tot},r}^{\pi^+}/\sigma_{\text{tot},r}^{\pi^-}$ at 0.7–2 GeV on C, Ca, Ni, Sn, Pb^{4,5}; $\sigma_{\text{tot},r}^n$ at 1–7 GeV on $4 < A < 238$,¹²

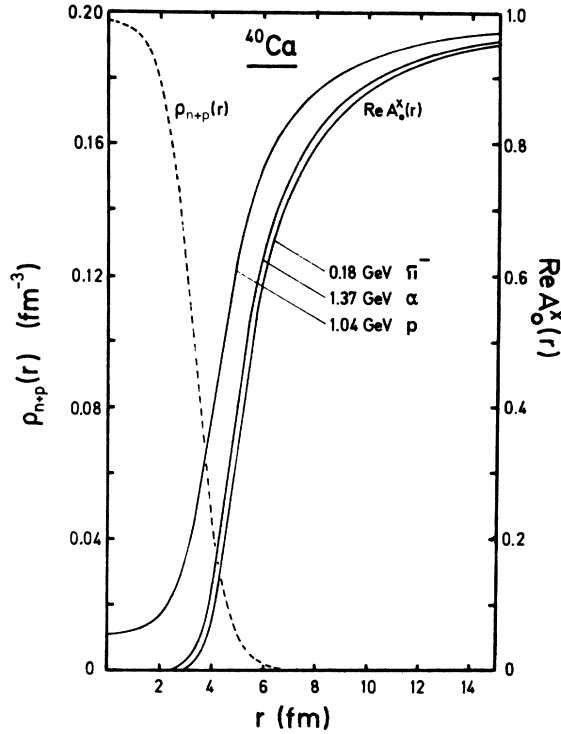


FIG. 1. Real part of the radial weight $A_0^x(r)$ [defined in Eq. (14)] for several projectiles bombarding ^{40}Ca (solid lines). Also shown (dashed line) is the nucleon point density distribution used in the calculation of $A_0^x(r)$ (see Sec. III).

and $\sigma_{\text{tot},r}^x$ ($x = \pi^-, K^-, \bar{p}$) at 20–60 GeV on C, Al, Sn, Pb.⁶ Commonly, the resulting $\rho_n(r)$ is quoted in terms of the parameters of a Fermi distribution or parameters derived therefrom (e.g., $\langle r^2 \rangle^{1/2}$).

Let us assume that a neutron density $\rho_n(r)$ has been found which is consistent with the measured σ_{tot}^x or $\sigma_{\text{tot},r}^x$. From the results of the preceding section it is obvious that any $\bar{\rho}_n(r) = \rho_n(r) + \Delta\rho_n(r)$ will also fit the data, provided the change $\Delta\sigma_{\text{tot}}^x$ or $\Delta\sigma_{\text{tot},r}^x$ [Eqs. (15) and (16)] caused by $\Delta\rho_n(r)$ is

less than the experimental error. Since this change equals the normalization integral [Eq. (10)] folded with a radial weight $\text{Re}A_0^x(r)$ or $B^x(r)$, total cross sections are only sensitive to $\rho_n(r)$ if these weight functions are not everywhere equal to 1 (otherwise one would just determine the total number of neutrons). This is actually the case for hadron-nucleus scattering, because here the projectile is strongly absorbed in the nuclear interior. As an example $\text{Re}A_0^x(r)$, Eq. (14), is displayed in Fig. 1 for various projectiles x and a ^{40}Ca target. The respective elementary forward amplitudes are listed in Table I. The densities $\rho_{n0}(r)$ and $\rho_{p0}(r)$ assumed for ^{40}Ca are identical with the ones of Ref. 7, where two-parameter Fermi distributions with $c_n = 3.296$ fm, $c_p = 3.364$ fm, $z_n = z_p = 0.585$ fm are used. As expected, $\text{Re}A_0^x(r)$ is zero or small in the nuclear interior and quickly approaches unity beyond the nuclear surface. For 180 MeV π^- , as an example, this rise takes place at approximately 5 fm, where the density has fallen to about 5% of its central value. It is obvious that there is a set of density distributions which yield the same calculated total cross section, the only condition being [see Eq. (15)] that all members are normalized to the same number of nucleons in the region *outside* the rise of $\text{Re}A_0^x(r)$. In the interior “black” region of the nucleus, where $\text{Re}A_0^x(r) = 0$, $\rho_n(r)$ is unbounded by σ_{tot} , except, of course, for the overall normalization.

Total cross sections therefore strongly depend on the number of nucleons outside the absorptive nuclear interior; thus σ_{tot}^x is not directly sensitive to the rms radius $\langle r^2 \rangle^{1/2}$ of $\rho_n(r)$. To obtain any information on $\langle r^2 \rangle^{1/2}$, it is absolutely necessary to restrict the shape of $\rho_n(r)$ by involving a model or by using independent information.

A model is necessarily introduced if $\rho_n(r)$ is given by a Fermi distribution. One can study the significance of the two free parameters by numerically evaluating the right hand side of Eq. (15). In this case, $\Delta\rho(r)$ is taken to be the change of the

TABLE I. Parameters of elementary forward amplitudes, Eq. (2).

Projectile	T_{lab} (GeV)	σ_n (fm ²)	ϵ_n	σ_p (fm ²)	ϵ_p
π^-^a	0.18	20.40	-0.05	6.90	0.13
π^-^b	0.84	1.98	-0.90	4.53	0.15
π^-^b	0.84	4.53	0.15	1.98	-0.90
π^-^b	1.58	3.61	-0.14	3.61	-0.38
p^c	1.04	4.04	-0.45	4.75	-0.10
α^d	1.37	10.70	0.29	10.70	0.29

^aReference 31.

^bReference 4, Table 8.

^cReference 11.

^dReference 32, p - α scattering at 345 MeV.

Fermi distribution if either z or $\langle r^2 \rangle^{1/2}$ is varied (with the normalization fixed). For a typical case (such as $\pi + {}^{40}\text{Ca}$, quoted above) it can be seen that a change in $\langle r^2 \rangle^{1/2}$ affects the integral $\text{Re}\langle A_0^*(r) \rangle_{\Delta\rho}$ much more than a corresponding change in z . This behavior is a consequence of the mathematical structure of a Fermi distribution. It makes possible the findings of most analyses where neutron rms radii are deduced from σ_{tot}^x or $\sigma_{\text{tot},r}^x$ data.

To appreciate the caveats associated with such analyses two recently published examples are discussed in the following. The first concerns a measurement of $\sigma_{\text{tot}}^{\pi^\pm}$ on ${}^{48,44,40}\text{Ca}$ in the (3,3) resonance region.⁷ Because of the uncertainty of the interaction model and the influence of the Coulomb interaction, isotopic differences between cross sections measured with pions of the same charge state are chosen as observables. If the isotopes ${}^{40,48}\text{Ca}$ are compared, four distributions $\rho_n({}^{40}\text{Ca})$, $\rho_p({}^{40}\text{Ca})$, $\rho_n({}^{48}\text{Ca})$, $\rho_p({}^{48}\text{Ca})$ are involved. Using two-parameter Fermi distributions, all eight parameters are fixed to values in accordance either with elastic electron scattering or Hartree-Fock calculations, except two, which were chosen as the isotopic differences ΔR_n , ΔR_p between the rms radii of the neutron and proton distributions, respectively. ΔR_n and ΔR_p are adjusted to fit the π^- and π^+ data. This procedure leads to $\Delta R_n = 0.14 \pm 0.05$ fm and a ΔR_p , which is consistent with elastic electron scattering. The corresponding ${}^{48}\text{Ca}$ neutron point density $\rho_n(r)$ is shown as a dashed line in Fig. 2.

Giving up the parametrization of $\rho_n(r)$ as a Fermi distribution, any $\tilde{\rho}_n(r) = \rho_n(r) + \Delta\rho_n(r)$ would also be acceptable, if only $\Delta\rho_n(r)$ yields $\Delta\sigma_{\text{tot}}^{\pi^\pm} \sim 0$, according to Eq. (15). An example for such a $\tilde{\rho}_n(r)$ is shown as a solid line in Fig. 2. The insert in Fig. 2 shows the isotopic $\sigma_{\text{tot}}^{\pi^\pm}$ difference measured⁷ and calculated with the distributions $\rho_n(r)$ and $\tilde{\rho}_n(r)$, keeping the remaining nucleon distributions in ${}^{40}\text{Ca}$ and ${}^{48}\text{Ca}$ fixed. It can be seen that it is impossible to distinguish between the two ${}^{48}\text{Ca}$ neutron distributions by means of the measurement. Nevertheless, the corresponding ΔR_n for the two cases are different by more than 3 times the error ± 0.05 fm originally quoted.⁷

We wish to point out that we do not consider $\tilde{\rho}_n(r)$ in Fig. 2 to be physically "reasonable." On the other hand, it is a difficult task to state the conditions of physical acceptability of the radial shape of neutron distributions. This may explain why none of the papers on neutron densities quoted so far³⁻¹³ are concerned with the reason for not considering densities like the above $\tilde{\rho}_n(r)$. To make things worse, the situation of Fig. 2 represents a favorable case, because first, we require $\Delta\sigma_{\text{tot}}^{\pi^\pm} \sim 0$ although $\Delta\sigma_{\text{tot}}^{\pi^\pm}$ may well be of the order

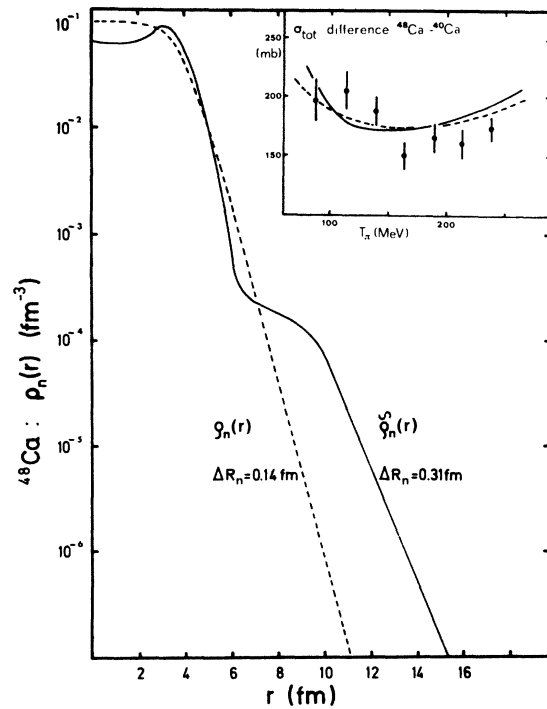


FIG. 2. Two different neutron density distributions for ${}^{48}\text{Ca}$. In the insert the ${}^{48}\text{Ca}$ - ${}^{40}\text{Ca}$ π^- total cross-section differences are calculated with these two distributions keeping the remaining nucleon distributions in ${}^{48}\text{Ca}$ and ${}^{40}\text{Ca}$ fixed. The data are from Ref. 7.

of the experimental uncertainties, and second, one can apply a similar manipulation also to the neutron distribution in ${}^{40}\text{Ca}$. It also has been shown²⁹ that it can be insufficient to use Fermi-type proton distributions $\rho_p(r)$. There is no indication of this in the analysis of $\sigma_{\text{tot}}^{\pi^\pm}$ on ${}^{40,48}\text{Ca}$ under discussion,⁷ since the resulting ΔR_p is consistent with the accepted value. In general, however, it seems advisable that proton distributions introduced in such an analysis should rather be the true ones (obtained, e.g., from a model-independent analysis of elastic electron scattering¹⁶). We conclude that parameters like ΔR_n extracted from $\sigma_{\text{tot}}^{\pi^\pm}$ data are subject to a large systematic error which can only be reduced if (physically justified) constraints are imposed on the radial densities. However, it is correct to reverse the logic and to use experimental data as a test for theoretical predictions of radial densities. The inconsistency between experimental isotopic $\sigma_{\text{tot}}^{\pi^\pm}$ differences and Hartree-Fock predictions for $\rho_n(r)$ which has been found⁷ is therefore *not* removed by the present considerations.

As a second example, we would like to scrutinize a measurement⁴ of $\sigma_{\text{tot},r}^{\pi^\pm}$ on C, Ca, and Pb from 0.7 to 2 GeV. The elementary amplitudes $f_{\pi n}$ and $f_{\pi p}$ differ from each other in this energy re-

gion which causes the data to be sensitive to differences between $\rho_n(r)$ and $\rho_p(r)$. Possible insufficiencies of the interaction model are this time suppressed by considering the ratio $\gamma = \sigma_{\text{tot},r}^{\pi^-} / \sigma_{\text{tot},r}^{\pi^+}$. We use the formalism developed in Sec. II to express the dependence of γ on the difference $\Delta\rho(r) = \rho_n(r) - \rho_p(r)$ between the neutron and the proton density. From Eq. (16) one finds

$$\gamma - 1 \cong \frac{\sigma_{r,n} - \sigma_{r,p}}{\frac{1}{2}(\sigma_{\text{tot},r}^{\pi^+} + \sigma_{\text{tot},r}^{\pi^-})} \langle B^r(r) \rangle_{\Delta\rho}, \quad (21)$$

where $\sigma_{r,\pm n}$ are the respective elementary total cross sections. The radial weight $B^r(r)$ [Eq. (17)] is displayed for various cases in Fig. 3. The corresponding elementary amplitudes are listed in Table I. The intrinsic densities assumed for ^{40}Ca and ^{208}Pb are two-parameter Fermi distributions. The parameters for ^{40}Ca have already been quoted; the ones for ^{208}Pb are¹⁴ $c_n = c_p = 6.542$ fm and $z_n = z_p = 0.549$ fm. The ^{12}C densities have been calculated from single particle wave functions generated in a Woods-Saxon potential requiring agreement with data on separation energies and elastic elec-

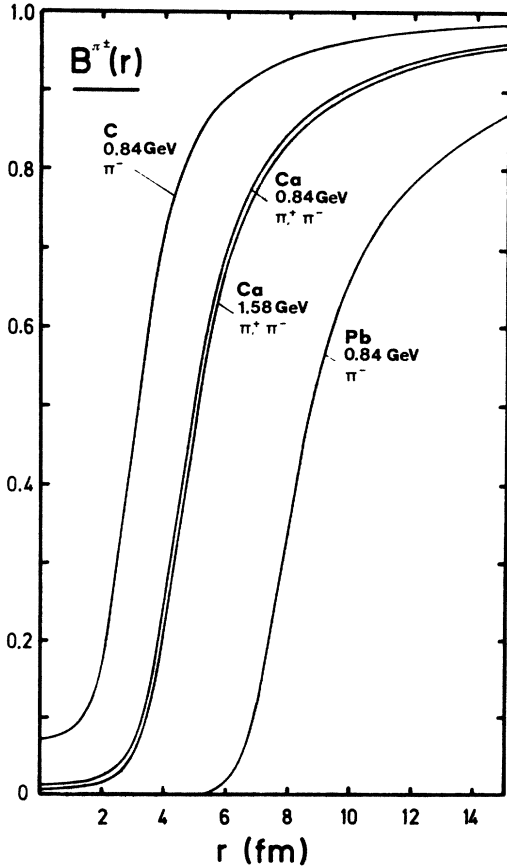


FIG. 3. Radial weight $B^r(r)$ [defined in Eq. (17)] for π^{\pm} bombarding C, Ca, and Pb (see Sec. III).

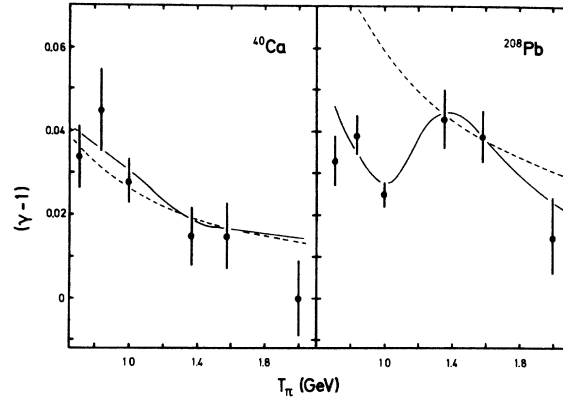


FIG. 4. Deviation from unity of the π^-/π^+ total reaction cross-section ratio γ as a function of bombarding energy for Ca and Pb. The dashed curve [Eq. (22)] represents the Coulomb effect alone. The solid curve [sum of Eqs. (21) and (22)] in addition contains the effect of the strong interaction. The data are taken from Ref. 4.

tron scattering.³⁰ As is seen from Fig. 3, $B^r(r)$ exhibits the same general behavior as $\text{Re}A_0^r(r)$ of Fig. 1. Note, that in our approximation γ is independent of the real part of the elementary amplitude which is significant since this quantity is often badly determined. $B^r(r)$ (Fig. 3) is practically independent of the charge state of the projectile [this fact has been used in the derivation of Eq. (21)] and the bombarding energy. Since projectiles of different charge are compared in γ , the Coulomb interaction causes an additional effect which is estimated according to Eq. (20):

$$(\gamma - 1)_{\text{Coul}} \cong \frac{4\delta}{(1 - \delta)^2}. \quad (22)$$

The "black-sphere-equivalent" radius occurring in δ [Eq. (2) of Ref. 26] has been arbitrarily fixed to the radius R where $B^r(R) = 0.2$. In Fig. 4 we compare our model to the data.⁴ The solid line corresponds to the sum of Eqs. (21) and (22), while the Coulomb contribution alone, Eq. (22), is marked by a dashed line. Several points become clear. First, our crude model describes the measurements surprisingly well, thus suggesting that many of the corrections taken into account in the original analysis⁴ are of minor significance. Second, the nuclear part of the observable is negligible for the isoconjugate ^{40}Ca and shows up in ^{208}Pb only because there are many more neutrons than protons. Third, the contribution of the strong interaction which contains the information on the matter distribution is obscured by purely electromagnetic effects, even at these high bombarding energies. It is therefore most important that all approximations of introducing the Coulomb force

into the interaction model (e.g., charge form factors, relativistic effects) be carefully checked, before reliable nuclear matter information can be extracted from the data.

We conclude this section by noting that we are not aware of any investigation of $\rho_n(r)$ by proton or α total cross sections, say in the GeV range, although these projectiles are as well suited as pions for this purpose. In addition, due to differences in the radial weights $\text{Re}A_0^x(r)$ (Fig. 1) cross-section data obtained with different projectiles x are complementary and should simultaneously be used in an analysis.

IV. DIFFERENTIAL CROSS SECTION

The previous section was addressed to total cross sections as a possible source of information about $\rho_n(r)$. Alternatively, cross-section measurements of elastic hadron-nucleus scattering have also been analyzed in terms of $\rho_n(r)$. It is appropriate to briefly touch upon some consequences of the results of Sec. II with respect to the elastic differential cross section [Eq. (5)]. We shall pass over the scattering of p and α at relatively low energies^{9,13} where $\rho_n(r)$ has to be extracted from an optical potential, as well as the scattering of π^\pm below the (3, 3) resonance⁸ for which a reliable parameter-free description is lacking at present. Rather, we are interested in the scattering of p or α around 1 GeV,^{10,11} which is satisfactorily described by the Glauber model.

Unfortunately, the connection between $\Delta\rho_N(r)$ and the corresponding change in the differential cross section is not as transparent as in the case of σ_{tot}^x and $\sigma_{\text{tot},r}^x$. Some facts, however, follow directly from an inspection of the momentum expansion of $\Delta F_x(q)$, Eq. (13). First, with increasing momentum transfer q , gradually higher moments $\langle r^n \rangle^{1/n}$ of $\Delta\rho_N(r)$ become important. Thus, an angular distribution which spans a range of q is sensitive to properties of the *shape* of $\Delta\rho_N(r)$ and not just to a normalization condition as σ_{tot}^x . Second, the contribution of any $2j$ th moment is again masked by a radial weight $A_j^x(r)$. As an example, the real and imaginary parts of $A_j^x(r)$ ($j \leq 3$) for 1.37 GeV α scattering from ^{40}Ca are displayed in Fig. 5. Note that radial weights for different moments are quite similar and that the "black" region persists for all j . Thus, again $\rho_n(r)$ is not determined in the nuclear interior ($r \leq 3$ fm), even by scattering at large momentum transfer. It should be remembered that the useful range of q is limited by the interaction model which becomes unreliable for large q because higher terms in the multiple scattering expansion become dominant.

In principle, angular distributions of the differ-

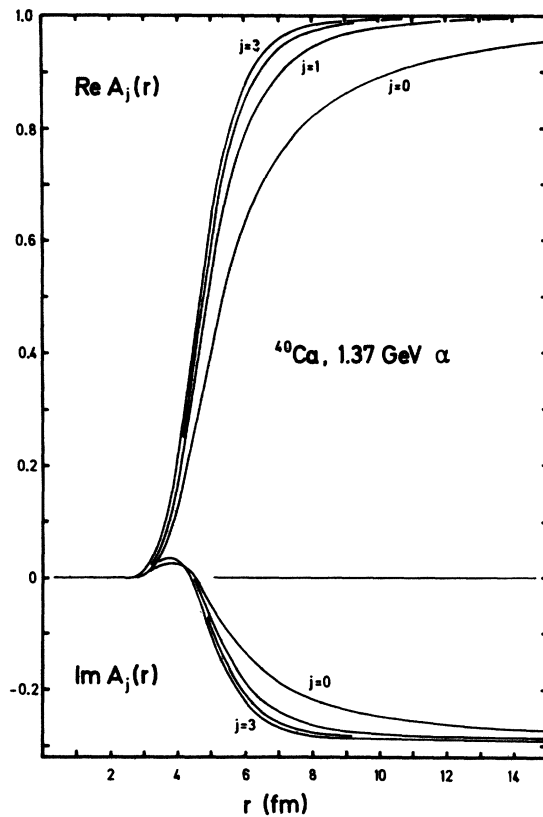


FIG. 5. Radial weight $A_j^\alpha(r)$ ($j=0, 1, 2, 3$) [defined in Eq. (14)] for 1.37 GeV α bombarding ^{40}Ca (see Sec. IV).

ential elastic cross section offer the possibility of an analysis which is free of a specific model for $\rho_n(r)$. One such method was originally introduced for the analysis of elastic electron scattering¹⁶ and was later applied to high-energy proton scattering.¹⁸ The idea is to represent $\rho_N(r)$ by a sum of Gaussians (SOG) centered at random radii r_j with amplitudes determined from a fit to the data. The method is not completely model independent since physical arguments are needed to fix the width of the Gaussians. If, in the analysis of hadron-nucleus scattering the SOG parametrization is chosen for $\rho_N(r)$ one has to appreciate the following. Each Gaussian in the sum couples values of $\rho_N(r)$ for a range of radii (in the case of Ca for example, the 10% width used for the Gaussians is ~ 3.5 fm). For the sake of the argument we assume that the nucleus has a completely black inner region. The coupling of $\rho_N(r)$ at different radii then produces a fake sensitivity of the calculated observables on $\rho_N(r)$ inside the black region. Such a parametrization, therefore, may not be appropriate for probes that lead to strongly varying weight functions like those shown in Figs. 1, 3, and 5. This difficulty becomes very serious in

another analysis of high-energy proton scattering,¹⁹ which is also claimed to be model independent with respect to $\rho_N(r)$. There, the profile function [which depends on $S_N(b)$, Eq. (4)], rather than $\rho_N(r)$, is described by a sum of step functions at random impact parameters b_j with amplitudes determined by a fit to the data. In such a parametrization each step function j introduces an inherent coupling of $\rho_N(r)$ in the range $b_j < r < \infty$. This incorrectly suppresses the effects of the shielding of the nuclear interior by strong absorption. Future analyses along these lines should try to accommodate these peculiarities which typically occur with strongly absorbed probes.

V. SUMMARY

The extraction of information on the nuclear neutron distribution from the scattering of strongly interacting projectiles suffers from the following difficulties. First, a reliable model has to be found for the description of scattering in terms of the elementary projectile-nucleon interaction. At present, there is no case where this task has been accomplished with no reservations. Second, accurate knowledge of the elementary amplitudes is required. To date, there are considerable uncertainties as, e.g., for the nucleon-nucleon amplitude at energies around 1 GeV and above. Third, $\rho_p(r)$ has to be known and fourth, some parametrization of $\rho_n(r)$ has to be chosen.

The present investigation is devoted to this latter difficulty. Using the Glauber model, we find that changes of $\rho_n(r)$ influence the calculated cross sections only if they occur outside the strongly absorptive nuclear interior. The total cross section, in particular, depends on the total number of nucleons outside this absorptive region. From this quantity one *can* deduce the rms radius of

$\rho_n(r)$, provided additional conditions are imposed on $\rho_n(r)$. Such conditions should come from physical arguments; it is questionable to introduce them by restricting the nucleon distributions to a simple mathematical form, as in the past has been common practice. This is exemplified by a discussion of the neutron distributions in Ca isotopes.

Sometimes it may be helpful to assay how strongly the observables depend on given properties of the nucleon distributions. On the basis of the simple model derived in this paper, this is done for a measurement of ratios of π^+/π^- total reaction cross sections.

We arrive at the conclusion that it is difficult to derive independent information on the neutron or matter distribution from total cross sections only. We rather recommend that such data be used either as complementary input in analyses simultaneously taking into account *all* of the available information on a given nucleus, or as one possible test of a theoretical prediction of the matter distribution.

Also discussed are angular distributions of the elastic differential cross section. In comparison to total cross sections, we show that more information can be expected from an analysis of measurements at varying momentum transfer. However, no matter how large the momentum transfer, differential cross-section data (like total cross sections) are insensitive to the matter distribution in the nuclear interior. We also critically review previous attempts to parametrize $\rho_N(r)$ free of a particular model assumption.

Finally, it is a pleasure to acknowledge many profitable comments by Dr. M. D. Cooper, Dr. L. Knutson, Dr. G. R. Plattner, Dr. R. Redwine, Dr. F. Roesel, Dr. I. Sick, Dr. D. Trautmann, and Dr. R. Viollier.

¹I. Sick, J. B. Bellicard, J. M. Cavedon, B. Frois, M. Huet, P. Leconte, A. Nakada, Phan Xuan Hô, S. Platchkov, P. K. A. deWitt Huberts, and L. Lapi-kás, *Phys. Rev. Lett.* **38**, 1259 (1977).

²H. Rebel, in *Proceedings of the Second Nuclear Physics Conference of the EPS: Radial Shape of Nuclei*, edited by A. Budzanowski and A. Kapuścik (Jagellonian U.P., Cracow, 1976), p. 164.

³G. D. Alkhazov, R. Beurtey, A. Boudard, G. Bruge, H. Catz, A. Chameaux, P. Couvert, J. L. Escudié, J. M. Fontaine, M. Garçon, J. Guyot, D. Legrand, J. C. Lugol, R. M. Lombard, M. Matoba, and Y. Terrien, *Phys. Lett.* **67B**, 402 (1977).

⁴B. W. Allardyce, C. J. Batty, D. J. Baugh, E. Friedman, G. Heymann, M. E. Cage, G. J. Pyle, G. T. A. Squier, A. S. Clough, D. F. Jackson, S. Murugesu, and V. Rajaratnam, *Nucl. Phys.* **A209**, 1 (1973).

⁵E. H. Auerbach, H. M. Qureshi, and M. M. Sternheim, *Phys. Rev. Lett.* **21**, 162 (1968).

⁶C. J. Batty and E. Friedman, *Nucl. Phys.* **A179**, 701 (1972).

⁷M. J. Jakobson, G. R. Bureson, J. R. Calarco, M. D. Cooper, D. C. Hagerman, I. Halpern, R. H. Jeppeson, K. F. Johnson, L. D. Knutson, R. E. Marrs, H. O. Meyer, and R. P. Redwine, *Phys. Rev. Lett.* **38**, 1201 (1977).

⁸G. Dugan, S. Childress, L. M. Lederman, L. E. Price, and T. Sanford, *Phys. Rev. C* **8**, 909 (1973).

⁹G. M. Lerner, J. C. Hiebert, L. L. Rutledge, C. Papanicolas, and A. M. Bernstein, *Phys. Rev. C* **12**, 778 (1975).

¹⁰G. D. Alkhazov, T. Bauer, R. Bertini, L. Bimbot, O. Bing, A. Boudard, G. Bruge, H. Catz, A. Chameaux, P. Couvert, J. M. Fontaine, F. Hibou, G. J.

- Igo, J. C. Lugol, and M. Matoba, Nucl. Phys. A280, 365 (1977).
- ¹¹G. D. Alkhazov, T. Bauer, R. Beurtey, A. Boudard, G. Bruge, A. Chameaux, P. Couvert, G. Cvijanovich, H. H. Duhm, J. M. Fontaine, D. Garreta, A. V. Kulikov, D. Legrand, J. C. Lugol, J. Saudinos, J. Thirion, and A. A. Vorobyov, Nucl. Phys. A274, 443 (1976).
- ¹²V. Franco, Phys. Rev. C 6, 748 (1972).
- ¹³G. M. Lerner, Nucl. Phys. A205, 385 (1973).
- ¹⁴C. W. de Jager, H. de Vries, and C. de Vries, At. Data Nucl. Data Tables 14, 479 (1974).
- ¹⁵L. S. Kisslinger, R. L. Burman, J. H. Koch, and M. M. Sternheim, Phys. Rev. C 6, 469 (1972).
- ¹⁶I. Sick, Nucl. Phys. A218, 509 (1974).
- ¹⁷I. Brissaud and M. K. Brussel, J. Phys. G 3, 481 (1977).
- ¹⁸I. Brissaud and M. K. Brussel, Phys. Rev. C 15, 452 (1977).
- ¹⁹R. J. Lombard and C. Wilkin, Lett. Nuovo Cimento 13, 463 (1975).
- ²⁰R. J. Glauber, *Lectures in Theoretical Physics* (Interscience, New York, 1959), Vol. 1, p. 315.
- ²¹J. Saudinos and C. Wilkin, Annu. Rev. Nucl. Sci. 24, 341 (1974).
- ²²G. D. Alkhazov, Nucl. Phys. A280, 330 (1977).
- ²³L. J. Tassie and F. C. Barker, Phys. Rev. 111, 940 (1958).
- ²⁴I. Sick and J. S. McCarthy, Nucl. Phys. A150, 631 (1970).
- ²⁵H. Lésniak and L. Lésniak, Nucl. Phys. B38, 221 (1972).
- ²⁶G. Fäldt and H. Pilkuhn, Phys. Lett. 46B, 337 (1973).
- ²⁷A. S. Clough, G. K. Turner, B. W. Allardyce, C. J. Batty, D. J. Baugh, J. D. McDonald, R. A. J. Riddle, L. H. Watson, M. E. Cage, G. J. Pyle, and G. T. A. Squier, Phys. Lett. 43B, 476 (1973).
- ²⁸C. Wilkin, C. R. Cox, J. J. Domingo, K. Gabathuler, E. Pedroni, J. Rohlin, P. Schwaller, and N. W. Tanner, Nucl. Phys. B62, 61 (1973).
- ²⁹R. M. Lombard, Lett. Nuovo Cimento 18, 415 (1977).
- ³⁰J. Heisenberg, J. S. McCarthy, and I. Sick, Nucl. Phys. A157, 435 (1970).
- ³¹G. Höhler and R. Strauss, Tables of pion-nucleon forward amplitudes, University of Karlsruhe, 1970 (unpublished).
- ³²P. Schwaller, B. Favier, D. F. Measday, M. Pepin, P. U. Renberg, and C. Sarre, CERN Report No. 72-13, 1972 (unpublished).